Interfaces
Vol. 38, No. 1, January–February 2008, pp. 5–25
ISSN 0092-2102 | EISSN 1526-551X | 08 | 3801 | 0005

informs

DOI 10.1287/inte.1070.0327

THE FRANZ EDELMAN AWARD
Achievement in Operations Research

Operations Research Advances Cancer Therapeutics

Eva K. Lee
School of Industrial and Systems Engineering and Center for Operations Research in Medicine and HealthCare, Georgia Institute of Technology, Atlanta, Georgia 30332, evakylee@isye.gatech.edu

Marco Zaider
Department of Medical Physics, Memorial Sloan-Kettering Cancer Center, New York, New York 10021, zaiderm@mskcc.org

Memorial Sloan-Kettering Cancer Center (MSKCC), the world's oldest private cancer center, seeks next-generation cancer treatment advances to enhance its ability to treat patients effectively by improving care and reducing costs. Using operations research approaches, our team has devised sophisticated optimization modeling and computational techniques for real-time (intraoperative) treatment of prostate cancer using brachytherapy (the placement of radioactive "seeds" inside a tumor). The resulting system offers significantly safer and more reliable treatment outcomes. In addition, it eliminates the need for preoperative simulation and postimplant dosimetric analysis, resulting in savings of hundreds of millions of dollars per year in the United States alone. Posttreatment quality of life is improved through drastic reduction (up to 45–60 percent) of complications. The reason for this is twofold: (a) treatment plans thus devised deliver less radiation to adjacent healthy structures, and (b) the ability to perform midimplant replanning eliminates the unavoidable discrepancies between planned and actual seed placement in the target. This has a profound impact on the cost of managing treatment-associated morbidity. The procedure uses approximately 20–30 percent fewer seeds and 15 percent fewer needles (used to place seeds inside the prostate gland). As a result, the operating-room time is shortened, and the entire procedure is less invasive. The system has the potential to establish standards and guidelines for cancer treatment quality control and quality assurance of the implantable plan.

Wide distribution of our system should allow consistent treatment planning across different clinics and significantly reduce variability in treatment plan quality. The next phase of this effort will expand the applicability of our system to other forms of brachytherapy, such as treatment of breast, cervix, esophagus, biliary tract, pancreas, head and neck, and eye.

Key words: prostate cancer; brachytherapy; optimization; integer program; treatment planning.

Prostate cancer has surpassed lung cancer as the most common form of cancer diagnosed in men and remains the second cancer killer of men in the United States. Of the estimated 220,000 new cases in 2007, 12 percent of the patients are expected to die from this malignancy. Worldwide, there are over 550,000 new cases per year, with the mortality rate exceeding 37 percent.

The treatment of prostate cancer, the outcome of which in terms of cause-specific survival remains uncertain, is often accompanied by untoward side effects. In outline, our work has two goals: (a) to reduce cancer-related mortality (by assuring full dosimetric coverage of the diseased site), and (b) to lessen treatment-associated morbidity (by careful dosimetric avoidance of normal, sensitive structures). As such, it is a showcase for "OR in the OR"—i.e., for the use of *operations research* (OR) to advance procedures performed in the *operating room*. Working with physicians at Memorial Sloan-Kettering Cancer Center (MSKCC),

we devised sophisticated optimization modeling and computational techniques for real-time intraoperative 3D treatment planning in brachytherapy (the placement of radioactive "seeds" inside a tumor). The resulting system can produce an optimized treatment plan in minutes (a *sine qua non* of the operating-room environment) rather than hours as with previous trial-and-error methods. In addition, the plans thus devised call for fewer seeds and needles, thus shortening the procedure time. Because fewer needles are inserted into the body during implantation, it is less invasive and patients are likely to recover faster.

The resulting treatment plans provide good tumor coverage (i.e., a tumoricidal dose of radiation is delivered to the malignancy), while maintaining minimal radiation exposure to critical healthy structures (urethra, rectum, and bladder). Thus, fewer patients are expected to require medications and interventions for management of side effects; and those who do experience such sequalae, generally require much shorter periods of intervention. This has a profound impact on both health-care costs and quality of life of the treated patients.

In 2005, about 30 percent of prostate cancer patients received brachytherapy treatment. It is expected that the proportion of patients choosing brachytherapy will increase because it generally causes less severe side effects compared to alternative treatments such as external beam radiation therapy (high-energy gamma rays) or surgery, which involves removal of the prostate. Both brachytherapy and surgery have similar recurrence rates; however, brachytherapy preserves the prostate gland and appears to be better in maintaining its functionality for sexual potency. This is of special concern to younger early-stage prostate cancer patients who still look forward to fathering children. Brachytherapy is most effective for patients with early-stage disease who, as a result of the trend in the United States for vigorous early screening, represent an increasing fraction among those diagnosed with prostate cancer.

There are two additional benefits of the OR-based intraoperative 3D computerized planning system described here. First, implants become less dependent on operator skill. Second, the potential exists to establish standards and guidelines for quality control and quality assurance.

The system can serve as a tool for training clinicians and residents on the procedure of implanting seeds. For example, because it allows on-the-fly dynamic dose reoptimization, errors in placing a few initial seeds can be corrected by accordingly reoptimizing the plan for the remaining seeds.

A system such as ours can serve as a basis for standardizing brachytherapy treatment planning in prostate cancer. It can also set a foundation on which to base automated computerized treatment planning for other brachytherapy procedures, e.g., breast, cervix, esophageal, brain, and sarcoma.

Last but not least, from an operations research perspective, the collaboration it engendered and the challenges it presented have led to advances in integer programming in both theoretical and computational areas.

In this paper, we describe the background of the treatment planning, the injection of sophisticated OR modeling and computational techniques into the planning procedure, the clear clinical significance and improvement, and the national distribution of the system. We also describe the broad impact of our work in terms of financial savings; quality-of-care and quality-of-life improvements; accessibility, training, quality assurance, and quality control across national clinics; and scientific advances.

Challenges—The Need to Advance Treatment Planning Design

In the United States, it is estimated that over 1.4 million new cancer cases are diagnosed each year (American Cancer Society 2006), and over half of the patients receive radiation treatment at some point during the course of their disease. The basic goals in radiation treatment are to deliver a lethal dose of radiation to malignant cells while limiting the dose to nearby healthy organs and tissues. Designing treatment plans to accomplish these goals is extremely demanding because it involves many physical and patient-related factors, including sensitivity of different tissue types to radiation, the direction and strength of the radiation sources, patient anatomy, and patient positioning during treatment.

Prostate Permanent Implants

Prostate cancer is the most common malignancy (in men) in the United States; it accounts for some 27,000 deaths each year. Routine treatment modalities for organ-confined disease are surgery and radiation therapy. While surgery can be very effective at eradicating disease confined to the prostate, it can also have severe side effects including loss of sexual potency and urinary incontinence. Radiation therapy can be delivered with external beams (teletherapy) of high-energy gamma rays, or by brachytherapy (permanent implantation of radioactive seeds or high dose rate treatment). Permanent implantation (hereafter referred to as brachytherapy) is becoming increasingly popular for two reasons. First, this mode of treatment can be compressed into a single-day surgical procedure. In contrast, teletherapy treatment involves repeated visits over a seven to nine week period. Second, brachytherapy allows the radiation dose to be better confined to the tumor, resulting in less damage to surrounding normal structures (e.g., rectum and bladder). Unlike teletherapy, permanent implants are not affected by setup and organ-motion errors.

Permanent-implant brachytherapy is particularly common in treating early-stage prostate cancer. In this modality, radioactive sources (Iodine-125 or Palladium-103) are permanently implanted in the prostate in a pattern designed to maximize the dose to the tumor while avoiding overexposure of the surrounding normal tissues. Available data (Blasko et al. 1996; Wallner et al. 1996, 1997; Zaider 2003) show similar five-year biochemical (based on PSA elevation) recurrence rates after brachytherapy and after surgery. However, when carefully implemented brachytherapy results in fewer side effects (involving loss of sexual potency and incontinence), and is more convenient for the patient (the entire procedure takes less than one day). Heretofore, the major limitation of radioactive-seed implants has been the difficulty of accurately placing 60–150 seeds within the prostate in a specified geometric pattern. However, with advances in implantation techniques, fairly accurate placement of seeds is now possible. Seed implantation is typically performed with the aid of a transrectal ultrasound (TRUS) transducer attached to a template consisting of a plastic slab with a rectangular grid of holes in it. The transducer is inserted into the rectum and the template rests against the patient's perineum. A series of transverse images are taken through the prostate, and the ultrasound unit displays the template grid superimposed on the anatomy of the prostate. Needles inserted in the template at appropriate grid positions enable seed placement in the target at planned locations. Figure 1 shows the needle template and TRUS placed inside the rectum. Despite such advances, deciding *where* to place the seeds remains a difficult problem. A treatment plan must be designed so that it achieves an appropriate radiation dose distribution to the target volume, while keeping the dose to surrounding normal tissues at a minimum.

Traditionally, to design a treatment plan, the patient undergoes a simulation ultrasound (US) or computerized tomography (CT) scan several days (or weeks) prior to implantation. During the scan, series of axial images with the grid superimposed are taken and saved. Prostate contours are drawn on each cut and the physicist-planner attempts—based on intuition and previous experience—to find a pattern of needle positions and seed coordinates along each needle that will yield an acceptable dose distribution. The resulting plan is graphically examined, with the intent to match the prescription axial isodose lines to the prostate contours and to limit the dose to the

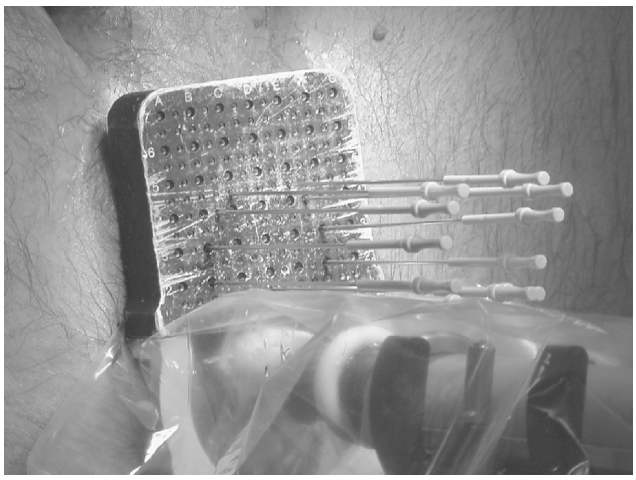

Figure 1: A needle template is used in a prostate permanent implant.

urethra and rectum. Typically, this requires a number of iterations and may take several hours to complete. This process is lengthy essentially because seed positions must be optimized in three dimensions, but can only be visualized (for any practical purposes) as a series of two-dimensional images. Each seed affects the dose not only in its own axial plane, but in adjacent planes as well, and thus every modification in the pattern of seeds must be examined globally. Such an approach (which is known as the preplan approach) has various limitations:

(1) The process requires manual inspection at each iteration; thus it is not only lengthy—taking several hours to complete—but only a small fraction of possible configurations can actually be examined.

(2) Images taken at a simulation session are often different from images obtained at the time of implantation. Thus, a plan (however optimal) designed on the basis of simulation images will not conform to the target boundaries determined in the operating room. Figures 2(a) and 2(b) illustrate the magnitude of this discrepancy; they show a preplan dose contour superimposed onto the actual prostate during the implantation in the operating room.

(3) Anatomical structures not visible on the ultrasound image (e.g., the pubic symphysis) may block the needles. This can be discovered only in the operating room and the treatment plan must then be modified by relocating the needles. Reoptimizing the plan manually is clearly not possible and ad hoc changes are the only option available. A similar problem occurs when the needle encounters the urethra or the bladder neck.

(4) Frequently, the prostate volume measured at simulation is different from the volume observed in the operating room, thus making the preplan invalid. In such a situation, one needs to add or remove seeds—again in an ad hoc fashion.

Discrepancies between the simulation-session data and the actual situation on the day of implantation can increase the likelihood of undesirable urinary and rectal-related side effects and poor local tumor control. Late severe toxicity (grade 3–4) (e.g., rectal fistulae and urethral strictures) have been reported,

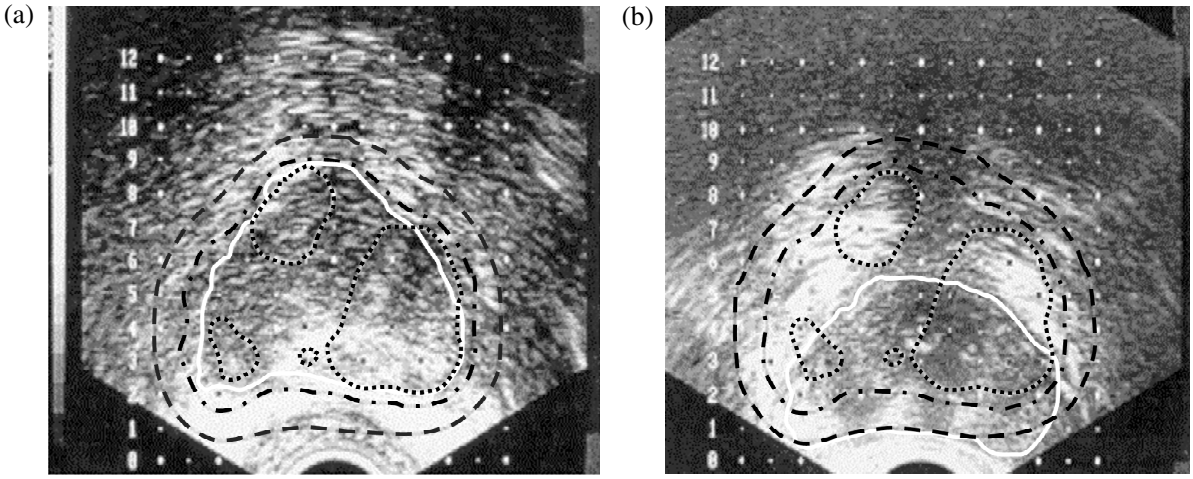

Figure 2: (a) This figure, which illustrates a preplan, shows adjacent axial ultrasound images with pretreatment isodose contours superimposed. Note the conformity of anatomy (prostate: white contour) and dosimetry (dashed lines = 50 percent; dashed-and-dotted lines = 100 percent; dotted lines = 150 percent; 100 percent = 144 Gy). The isodose lines are the results of an I^{125} plan. (Conformity is a measure of how well the prescription dose isodose curve conforms to the boundary of the planning target volume (PTV). The PTV includes the visible tumor volume plus a small margin to include potentially diseased cells that are not part of the visible tumor volume.) (b) This figure shows the adjacent axial operating-room–acquired images with pretreatment isodose contours. Note the lack of conformity of dosimetry and anatomy of the preplan isodose versus the prostate images acquired during the implantation session. The contours have the same meaning as in Figure 2(a).
Source. MSKCC.

while moderate (grade 2) urethral complications (e.g., urinary frequency and urgency necessitating medications for symptomatic relief) remain the most important limitations in prostate implants. Using current ad hoc and heuristic approaches, it is often physically impossible to reduce the radiation dose to the urethra without compromising the dose distribution to the prostate (Kleinberg et al. 1994, Zelefsky and Whitmore 1997). Kleinberg et al. (1994) have shown that urinary frequency and urgency will likely persist for up to 12 months after implantation and gradually resolve with time. Many practitioners have reported that this phenomenon continues for at least one to two years after implantation.

At MSKCC, we (Zelefsky et al. 2003) and others have shown that lower urethral doses were associated with fewer urinary symptoms after the brachytherapy procedure. Figure 3 shows recent data that highlight the important observation that the attainment of a limited urethral dose range (dose delivered to 20 percent of the urethra, $DU_{20} < 200$ Gy) is associated with a decreased incidence of grade 2 or higher complications, and our data suggest that achieving lower doses would reduce the risk of such complications.

Urinary side effects can have a significant impact on a patient's overall quality of life. While temporary urinary side effects may be inevitable for patients treated with prostatic implantation, it is plausible that with real-time intraoperative optimization techniques and on-the-fly dynamic dose-correction protocols (see below), these side effects will be further reduced without compromising local tumor control.

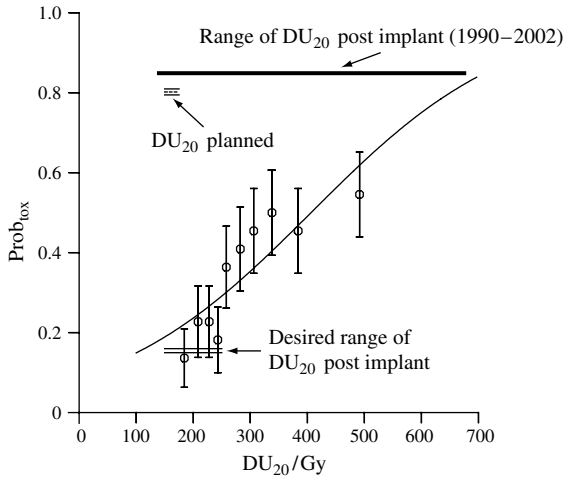

Figure 3: This graph shows the probability of grade 2 or higher urethral toxicity at 12 months after treatment, $\text{Prob}_{tox}(12 \text{ months})$, as a function of DU_{20} (i.e., 20 percent of the urethral volume is treated to a dose of at least DU_{20}). The disparity between planned and implemented doses is such that on average, $\text{Prob}_{tox}(12 \text{ months}) = 0.36$.

Solutions

Prior to our OR work, medical physicists had developed computer-aided iterative approaches and heuristic methods, such as simulated annealing and genetic algorithms, to aid in brachytherapy treatment planning in the operating room (Anderson 1993, Silvern et al. 1997, Silvern 1998, Sloboda 1992, Yu and Schnell 1996). While these methods can return feasible solutions, there are limitations on the type of clinical restrictions one can incorporate. In addition, because of their heuristic nature, the quality of resulting plans cannot be measured (i.e., how far they are from optimality). Unlike this previous work, our work utilizes advanced OR modeling and computational techniques, attacking this clinical problem from its root, and allowing medical physicists and clinicians to incorporate desirable clinical properties within the treatment models we develop (Gallagher and Lee 1997; Lee et al. 1999a, b; Zaider et al. 2000; Lee and Zaider 2001a, b, 2003a, b, 2004, 2006). Two primary goals drive our work: the ability to incorporate clinically significant constraints of any type, and the achievement of optimal solutions in OR-constrained time (i.e., rapid enough—within minutes—to enable usage in the operating room). The latter allows for intraoperative planning by clinicians, overcoming preplanning problems and allowing real-time alteration of plans because of unforeseen implantation problems. Ultimately, the resulting optimization system should be an important tool for biological (functional) optimization (Zaider et al. 2000; Lee and Zaider 2004, 2006).

Our Approach: Integer Programming Treatment Planning Model

Fundamentally, the treatment planning optimization problem for brachytherapy is a combinatorial problem. Our treatment model uses 0/1 variables to record placement or nonplacement of seeds in a prespecified three-dimensional grid of potential locations. In the

case of prostate cancer, the locations correspond to the projection of the holes in the template onto the region representing the prostate in each of the ultrasound images. If a seed is placed in a specific location, then it contributes a certain amount of radiation dosage to each point in the images. To facilitate modeling of the dose distribution, we select, from each image, a uniformly spaced sampling of points at which to measure radiation dosage. The density of the spacing is chosen at a level that is conducive to both modeling the problem accurately, and to ensuring that problem instances are computationally tractable. We have used spacing ranging from 2 mm to 10 mm, and have found 5 mm to be a reasonably good choice for the problems we have considered. The sample points in the images are referred to as *voxels* (volume elements).

Once the grid of potential seed locations is specified, we can model the total dose level at each voxel. For each voxel in each anatomical structure, we associate one binary variable and one continuous variable to capture whether or not the desired dose level is achieved, and the deviation of received dose from desired dose. These variables allow us to capture dose-volume relationships in the resulting treatment plans (e.g., x percent of structure K received no more than dose D) (Kutcher and Burman 1989, Lyman 1985). Constraints in the model include dosimetric constraints for the tumor and critical structures. Typically, the clinician will specify the "prescription dose" desired for the tumor volume; then lower and upper bounds for dose to all structures are stated in terms of percentages of prescription dose. For example, dose to the urethra should be less than 120 percent of prescription dose.

Typically, it is not possible to satisfy desired dose constraints at all points simultaneously. In part, this is due to the proximity of diseased tissue to healthy tissue. In addition, because of the inverse square distance factor in dose attenuation, the dose-level contribution of a seed to a point that is, for example, less than 0.3 units away, is typically larger than the target upper bound for the point. (Hence, the preprocessing techniques commonly mentioned in the integer programming literature cannot be applied directly to these dose constraints because this will result in assigning zero to all seed positions.)

However, it is possible—and clinically desirable—to incorporate dose-volume coverage constraints for the tumor within the model. For example, the clinicians often consider that it is acceptable if 95 percent of the tumor receives the prescription dose. While there is no mechanism to incorporate it within ad hoc and existing heuristic approaches to treatment planning, this guideline is commonly used in the clinical setting, and we can model it readily within our integer programming formulation.

In our work, we focus on two models. The first involves finding the maximum feasible subsystem in our MIP formulation. We do this by utilizing the 0/1 variables assigned to the voxels to compute the maximum number of tumor points that satisfy the specified bounds. An alternative model involves using continuous variables to capture the deviations of the dose level at a given tumor point from its target bounds and minimizing a weighted sum of the deviations.

To aid in reducing urinary and rectal toxicity, our approach involves the imposition of strict dosimetric-volume bounds on the urethra and rectum in both MIP models. In addition to the basic dosimetric constraints, and dose-volume constraints to ensure sufficient coverage to the tumor volume, we also incorporate other physical constraints desired by the clinicians into our MIP models. One could—if desired—constrain the total number of seeds and/or needles used, and employ multiple seed types having different radioactive strengths. We describe the integer programming formulation in the appendix.

Computational Advances

The treatment models present a very unique challenge to the OR community. Due to the inverse square distance factor in the attenuation of radiation, and the confinement of the radiation within a very small area, the dose matrix of the treatment model is *completely dense*, with coefficient magnitudes ranging from the order of tens to tens of thousands. Furthermore, none of the problem instances is tractable by existing commercial MIP solvers. While there have been tremendous advances on solution techniques for MIP (an NP-complete class of problems) in the past 50 years, much of the work has been motivated

and guided by large-scale instances involving sparse constraint matrices, which are common in most industrial applications. Dense MIP instances, as Cornéjols and Dwande (1999) describe, present a unique new challenge to the OR community, even when they involve only several hundreds of 0/1 variables with 20 constraints. Easton et al. (2003) subsequently provided solution strategies to solve dense market share instances to optimality via novel hypergraphic cutting planes and an aggregate branching scheme.

Table 1 illustrates the running time statistics for a patient case with 4,398 rows and 4,568 variables, running on the commercial MIP solver CPLEX V9.

In all patient cases that we tested, using various advanced strategies within CPLEX, we observed the computational bottleneck in which no feasible solutions were obtained and there was only marginal improvement in the LP objective value over an extended time. (This was also confirmed by one of the software founders.) This proved that, although OR provides a very flexible modeling environment to facilitate brachytherapy treatment planning, using the OR models in clinical practice would not be possible without a major computational breakthrough for solving these intractable MIP instances. Therefore, we developed novel computational techniques. These include: a matrix reduction and approximation scheme, a penalty-based adaptive primal heuristic, a specialized branching strategy, and cutting planes derived via hypergraphic structures (Lee and Zaider 2003a, Easton et al. 2003, Lee and Maheshwary 2008).

CPU secs. elapsed	Best IP obj.	Best LP obj.	Branch-and-bound nodes searched
Model 1			
15.35	—	6,915.5853	100
131.71	—	6,133.4341	1,000
1,407.58	—	6,132.9121	1,000
2,800.72	—	6,132.4741	2,620
7,672.30	—	6,131.6915	20,000
20,778.27	—	6,131.2541	110,000
71,988.54	—	6,130.8357	130,541
149,468.27	—	6,130.5719	1,000,000
202,766.38	—	6,130.4391	1,326,000
CPLEX added 274 cuts at the root node			

Table 1: The table data show solution statistics for Pt 1 running on CPLEX V9.0 on a Sun V20z, dual opteron 250 (2.4 GHz) with 4 GB RAM.

We briefly describe the computational strategies in the appendix. Easton et al. (2003) show the theoretical detail of the hypergraph. We incorporated these techniques within a branch-and-cut environment, yielding a powerful MIP solver that successfully solved the brachytherapy treatment planning instances to proven optimality. Perhaps more importantly, the system returns feasible plans (with good urethra dose limits) *within seconds that are within 95 percent of optimality*, and have superior clinical properties.

Clinical Outcome

By incorporating cutting-edge optimization techniques, the OR modeling paradigm offers the best accuracy in dose delivery while simultaneously lowering radiation to normal tissues. High-quality plans can be returned within seconds, thus opening up the opportunity for *real-time intraoperative 3D planning* (Lee et al. 1999a, b; Lee and Zaider 2001b, 2003a, b). This eliminates the need for a simulation session in which patients come in days or weeks in advance to have the US/CT images taken. It also eliminates the time-consuming task of generating operator-dependent treatment plans via iterative approaches prior to the actual implantation session. In addition, by designing treatment plans on the day of implantation, it overcomes the preplanning discrepancies mentioned earlier related to poor reproducibility of patient positioning (i.e., images taken for preplanning are often substantially different from images obtained at the time of implantation). It also overcomes target volume changes between the day of simulation and the day of implantation. Further, it allows for *on-the-fly intraoperative dynamic dose reoptimization* (IDDO) (Lee and Zaider 2001b, 2003b; Zelefsky et al. 2003), enabling clinicians to handle unforeseeable difficulties (e.g., when the needle encounters the urethra or the bladder neck) during implantation. The reoptimization capability serves as a quality-control method to ensure that the final implanted configuration meets the requirements of the desired dose distribution.

We developed an optimization tool that can incorporate any known constraints of clinical significance, and solve the problem in real time for use in the operating room. In comparison to traditional computer-aided approaches, and other ad hoc heuristic methods such as genetic algorithms, the system

we developed consistently returns plans with prescribed dose delivered to 98 percent of the prostate; it improves conformity ranges from 10–20 percent (thus reducing toxicity to normal tissue exterior to the prostate, such as the bladder and rectum); it reduces urethra dose by 23–28 percent; it reduces rectum dose by 15 percent; it uses approximately 20–30 percent fewer seeds and 15 percent fewer needles and results in an underdose of within 3 percent of the prescribed dose (Lee et al. 1999a, b; Lee and Zaider 2001a, 2003a; Zelefsky et al. 2003).

MSKCC set a leading example in implementing real-time intraoperative 3D treatment planning for prostate permanent implants (Zelefsky et al. 2003). Subsequently, new research frontiers were opened as a result of having a fast treatment planning engine with constraint incorporation capability (Zaider et al. 2000; Lee and Zaider 2001a, b, 2003b, 2004, 2006).

Reduction in Grade 2 Urinary Toxicity

Grade 2 urinary symptoms represent the most common toxicity after prostate brachytherapy. These side effects, which often necessitate alpha-blocker medications to control urinary frequency, urgency, and dysuria, as well as the occasional need for urologic evaluation for urinary retention and self-intermittent catheterization, impact substantially the quality of life of the treated patient. Many reports have corroborated the increased propensity for acute urethral toxicities after prostate brachytherapy, and these effects have been shown in clinical studies to have a detrimental impact on the quality of life (more than rectal side effects, which are generally minimal, or sexual dysfunction) when compared to surgery and external beam radiotherapy (Wei et al. 2002). For a procedure that is performed frequently in this country, occasionally by practitioners with limited experience, research advances pioneered at our institutions to achieve a consistent application of a limited urethral dose, decrease the operator dependency and reduce the influence of the learning curve associated with prostate brachytherapy, have important consequences both for clinical practitioners and for treated patients.

Tables 2 and 3 and Figures 4, 5, and 6 illustrate the toxicity reduction to the urethra and rectum; Table 2 compares the average urethral dose and the incidence of acute grade 2 urethral toxicity for two alternative treatment approaches (Lee and Zaider 2003b). *Using intraoperative 3D planning in the operating room, grade 2 urinary toxicity was reduced drastically by 45 percent in the first six months, and by 60 percent in months 6 to 12. This results in a very significant reduction in side effects for brachytherapy implants. Thus, fewer treated patients require medication to manage side effects.*

Planning technique	Average urethra dose Durethra/DPrescription dose	Percent of incidence of toxicity	
		<6 months	6–12 months
Preplanning ($n = 247$)	182%	85%	58%
Intraoperative 3D ($n = 182$)	143%	46%	23%
p-value		0.01	0.01

Table 2: The table data show the incidence of acute grade 2 urinary toxicity during the first 6 months and from 6 to 12 months after the procedure, as well as the average urethral dose (expressed as a percentage of the prescription dose) for the two types of treatments (Lee and Zaider 2003b).

In Table 3 and Figure 4, Zelefsky et al. (2003) contrast the long-term effect of urethra toxicity and grade 2 symptoms of 247 preplan patients (treated between 1988 and 1996) versus 248 intraoperative 3D patients treated at MSKCC since 1998. Table 3 shows statistics on the dose-distribution comparison. Reduction of urethra dose is drastic.

Figure 5 provides additional evidence of the success of the intraoperative 3D planning; it shows a uniform urethral dose reduction to patients who have

Outcome	Preplan transperineal implantation ($n = 134^*$)	Real-time intraoperative 3D conformal ($n = 245^*$)	P
Target V_{100} (%)	89	94	<0.0001
Rectal maximal dose (% of prescribed dose)	183	99	<0.0001
Urethra maximal dose (% of prescribed dose)	532	167	<0.0001

Table 3: The data show a multivariate analysis of outcome variables adjusted for implant volume and total activity. Target V_{100} data are presented as percentage of prostate covered by the prescription dose; values shown represent median values. *The postimplant urethra dose was measured in 134 of 247 patients; similarly, it was measured in 245 of 248 patients.

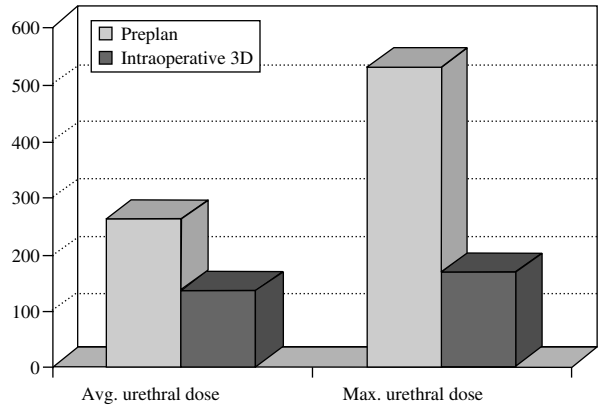

Figure 4: This figure contrasts the postimplant urethral dose, measured four hours after implantation, of a preplan and an intraoperative 3D plan. The vertical axis indicates the percentage of prescription dose (Zelefsky et al. 2003).

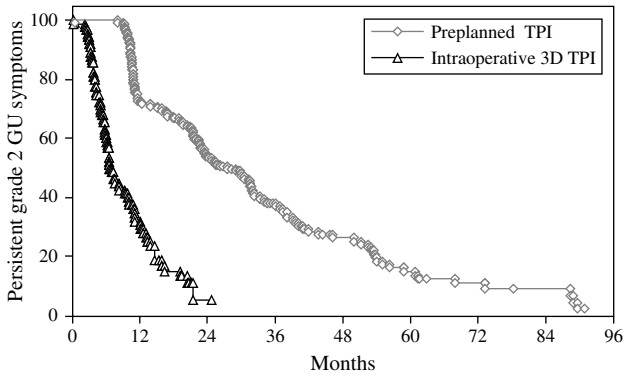

Figure 6: This figure shows time of resolution of grade 2 urinary symptoms; it compares 116 preplan patients and 111 patients treated using real-time intraoperative 3D plans.
Source. Dr. M. J. Zelefsky at MSKCC.

received prostate seed implants since their introduction in 1998.

It is also critical to compare the duration of side-effect management for patients in the two groups who experienced similar grade 2 urinary toxicity. Figure 6 plots the time of resolution of urinary symptoms. The results show a clear improvement using intraoperative 3D planning, with the average time of resolution being 9 months versus 32 months, respectively. *This translates to hundreds of millions of dollars in savings in health-care costs for medication and symptom management, and more importantly, a better quality of life for treated patients.*

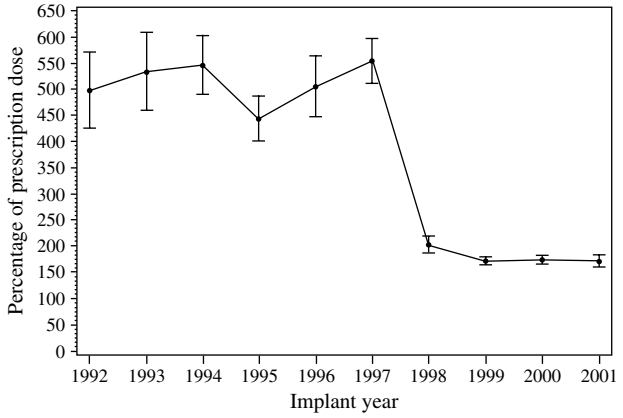

Figure 5: This graph shows the maximal urethral dose expressed as a percentage of the prescribed dose depicted over time. A significant decrease of the urethral dose was observed in 1998 with the introduction of the intraoperative 3D optimization technique. Excess urethral dose is directly proportional to grade 2 urinary toxicity experienced by treated patients.

Dynamic Planning and Reoptimization

Using the system we developed, it is possible to dynamically reoptimize plans during implantation to account for actual implanted seed positions and needle-induced swelling to the prostate during implantation (Figures 7 and 8). As alluded in our 2003 clinical study, while intraoperative planning eliminates the preoperation simulation procedure, intraoperative dynamic dose reoptimization, *IDDO, serves as a quality control on the resulting dose distribution and eliminates the need for a postimplant CT scan* (*an important cost-savings benefit*).

Figure 7 illustrates the magnitude of dose discrepancy observed in postimplant analysis using a random group of 17 patients treated at MSKCC via intraoperative 3D planning. It highlights the percentage of urethral volume covered by 150 percent of the prescription dose (planned versus assessed at postimplant evaluation) and also 200 percent of the prescribed dose (postimplant evaluation; the planned percentage volume was always zero). These data demonstrate that with a needle-based optimization approach, variations from the planned urethral dose and the actual dose delivered are frequently observed, and highlight the need to periodically readjust the plan to account for the real-time position of seeds already implanted to provide optimal postimplant

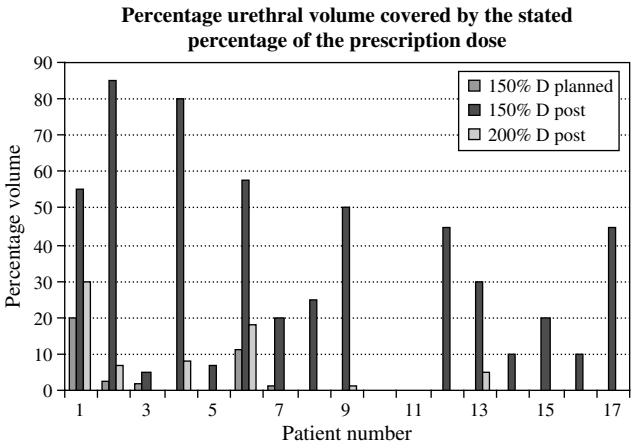

Figure 7: This graph illustrates the variability in postimplant urethral dose in a sample of 17 patients.

dosimetric measurement upon completion of seed implantation.

Figure 8 illustrates the additional postimplant urethral dose reduction when using real-time intraoperative planning with and without IDDO. Unlike other planning techniques, the MIP system allows for a very tight dose restriction set on the urethra ($\geq$100 percent and $\leq$120 percent) (Lee and Zaider 2001b, 2003b). Note also that although real-time intraoperative planning sets the urethra upper dose to be $\leq$120 percent, upon implantation and seed displacement (as needles are removed from the prostate), the actual postimplant dose exceeds the planned dose bound of 120 percent. By periodic readjustment and reoptimization of seed locations during implantation, one can achieve the desired postimplant dose limits.

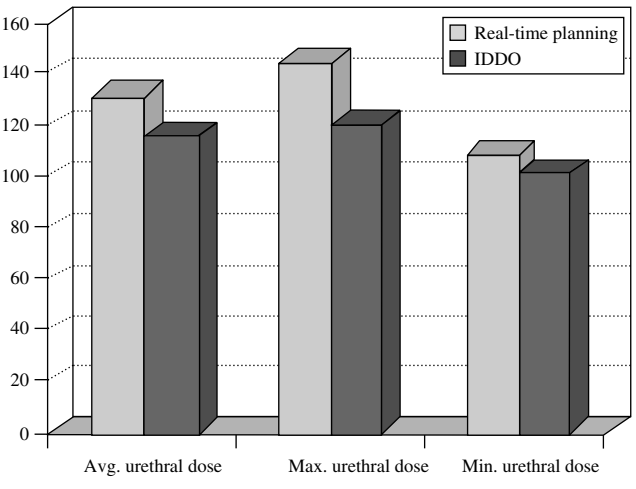

Figure 8: This graph illustrates the benefit of IDDO in reducing the postimplant dose to the urethra.

Beyond Real-Time Intraoperative Planning and Dynamic Dose Reoptimization

Subsequent to the computational breakthrough that allowed real-time planning, the need to design plans days in advance of implantation ended. Planning now may occur in the operating room immediately prior to implantation. This opens the door to new avenues of research on treatment outcome.

Tracking Tumor Shrinkage and Seed Displacement (4D-Planning: Planning with Temporal Information)

A plan that is based on the swollen prostate volume at implant time may be conformal, but it will not provide good dosimetry over time as edema resolution occurs. In particular, the dose received by the urethra and rectum will exceed the planned limits. While clinical studies have confirmed these discrepancies (Moerland et al. 1997; Prestidge et al. 1998; Waterman et al. 1998; Waterman and Dicker 1999; Waterman et al. 1997; Yue et al. 1999a, b), no one had previously considered planning based on more than a single-day snapshot of the tumor volume and surrounding anatomy. This is in part due to the daunting combinatorial optimization problem that one is faced with in designing plans—even plans that involve only the traditional single-day snapshot.

With our computational breakthrough, we demonstrated on real patient data that by designing treatment plans based on a 30-day period, i.e., the time it takes a needle-induced swollen prostate to shrink back to its original size (Waterman et al. 1998)—enforcing dose restrictions at regular intervals over this time horizon (thus expanding the size of our MIP instances by many fold)—there is a potential additional dose reduction of 20 percent to urethra and rectum, and improved tumor conformity over 21 percent (Lee and Zaider 2001a). These improvements translate to lower normal tissue side effects for prostate cancer patients. Figure 9 illustrates that

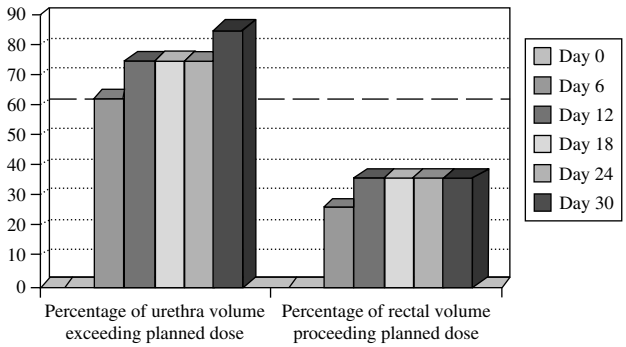

Figure 9: This figure shows the percentage of urethra and rectal volume exceeding the planned dose over a 30-day horizon after implantation when using a single-day's data (the day of implantation) for planning. Initially, on Day 0, the excess dose is zero, indicating that the seeds were placed appropriately according to plan. But due to tumor shrinkage and seed displacement over time, significant portions of both structures exceed target dose bounds at later times. In contrast, using 30-day information to design a treatment plan, the resulting plan has all percentages equal to zero because the plan constrains the dose distribution by considering shrinkage and seed displacement (Lee and Zaider 2001a).

dose to the urethra and rectum can be controlled well over an extended time period—without sacrificing local tumor control—by imposing dose-volume bounds for multiple periods. Using sophisticated OR techniques, our system remains today the *only system* that allows multiperiod planning capability and analysis. *This capability is of paramount importance. Using a preplan may underdose the tumor target and overdose the urethra and other critical structures. Using single-period OR-based planning may lead to overdose of the urethra as treatment begins, and the prostate shrinks to its normal size. Therefore, 30-day dose control is extremely important* (*as many clinical researchers have suggested*)*, and again we show the power of OR to be critical in designing such plans.*

Incorporating Biological Metabolite Information in Treatment Planning

Currently, prostate cancer is being treated as a homogeneous mass. With the advances in magnetic resonance spectroscopy (MRS), there is a need to incorporate the information it provides (e.g., the presence of aggressive cancer) within the planning process. We illustrated through real patient cases that by designing treatment plans that escalate dose in selected subvolumes (identified via MRS), tumor control probability can be improved from *65 percent to 95 percent* without increasing toxicity to the rectum, urethra, or bladder wall (Zaider et al. 2000; *New York Times* 2001; Lee and Zaider 2004, 2006). In addition to our OR model and computational engine, we designed a voxel transformation algorithm (a nonlinear mixed-integer program) to map the MRS biological information onto the treatment images. This allowed for biologically enhanced treatment, which facilitated targeted delivery of escalated dose and the potential to improve overall clinical outcome. Such planning is possible because our OR model has great flexibility in imposing dose constraints to achieve desired bounds at selected locations. It provides the capability to increase dose to tumor pockets, and limit dose to critical normal structures such as the urethra and rectum.

Transfer of Technology

The OR intraoperative 3D treatment planning system has been licensed to a medical software company, which has over 700 client clinics in the United States for radiation treatment. In Figures 10(a) and 10(b), we illustrate the treatment plans from the commercial system. The system is used in real time in the operating room during implantation.

Our system has functionality beyond the treatment of prostate cancer. Brachytherapy has been successfully used in treating cancers of the breast, eye, cervix, biliary duct, head and neck, esophagus, pancreas, and intravascular lesions. The commercial brachytherapy planning system has been used for prostate, breast, gynecological, and sarcoma implants.

Benefits

Cost Savings

Our system eliminates the cost of the pretreatment simulation session, including imaging, preplan treatment design by an expert planner, labor, and facility usage. Cost savings are estimated to be $5,000 per patient. This does not factor in further savings to the patient, e.g., costs of time off from work for the simulation session and hospital waiting time.

In the United States, there will be an estimated 218,890 new cases of prostate cancer in 2007. The American Brachytherapy Society (2005) statistics show that approximately 30 percent of patients are

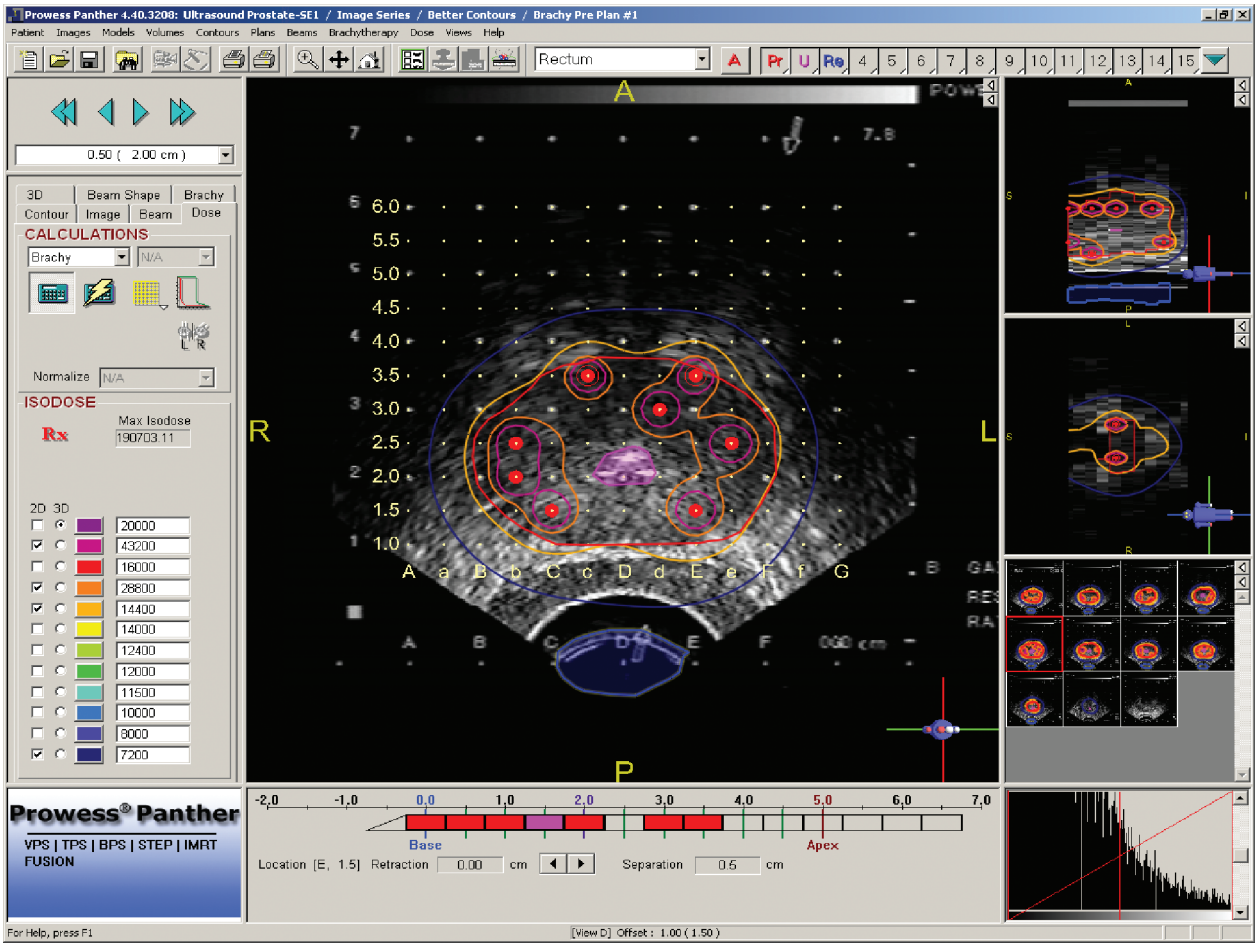

Figure 10a: This figure illustrates the commercial system. Note the excellent conformity of the OR plan. The brown isodose curve, representing points that receive 100% of the prescription dose, conforms well to the red curve, which delineates the boundary of the planning target volume.

treated using brachytherapy, 30 percent external beam radiation, 25 percent surgery, and 15 percent with other modalities. Thus, nationwide, when *all* clinics adopt intraoperative real-time planning, the potential annual cost savings would total 328 million dollars per year ($218{,}890 \times 0.3 \times 5{,}000$).

Moreover, observing the clinical trend, it is expected that the proportion of patients who choose brachytherapy will increase because its side effects are generally less severe when compared to external beam radiation therapy and surgery, and because of its effectiveness for early-stage diagnosis (*New York Times* 2006). Brachytherapy is most effective for early-stage diagnosis; this is the trend in the United States where annual physical examinations of male patients include vigorous early screening. Compared to surgery, brachytherapy has a similar five-year recurrence rate (20 percent); however, it preserves the organ and its functionality for sexual potency. The latter is of special concern to younger early-stage prostate cancer patients who still look forward to fathering children.

Real-time intraoperative treatment planning will provide significant savings in countries other than the United States. In 2000, the incidence rate of prostate cancer was roughly 550,000 worldwide; traditionally,

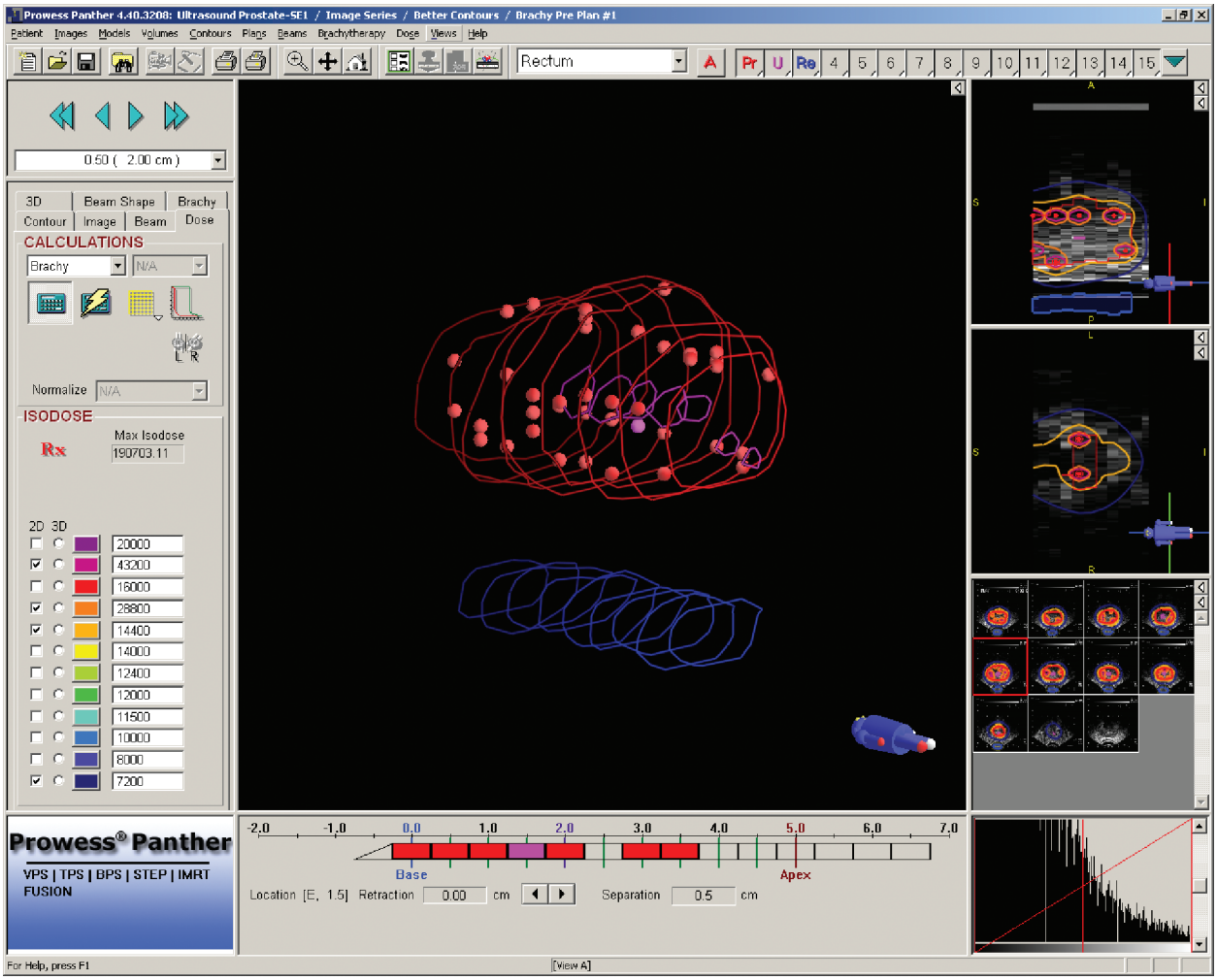

Figure 10b: This figure shows the 3D seed locations inside the prostate, as determined via the OR-based treatment planning system. The blue structure is the rectum, and the purple indicates the urethra.

brachytherapy is used more widely in other parts of the world because of its treatment convenience (a half-day procedure) and relatively low side effects.

Intraoperative planning with dynamic dose correction provides superior postimplant dose analysis and has eliminated the traditional postoperation CT scan. *This contributes to additional savings of roughly 131 million dollars per year for brachytherapy treatment of prostate cancer alone*.

Our OR planning system results in a reduction of 20–30 percent of seeds compared with traditional preplanning methods. Each seed costs approximately $20–$50, and each implantation involves 60–200 seeds. Assuming that an average of 100 seeds are implanted per patient via preplanning, with a cost of $30 per seed, then a 20 percent reduction in seed usage by applying our system would lead to a per-patient savings of $600, and an annual cost savings of $39 million nationwide ($218,890 \times 0.3 \times 600$). There is no additional labor cost because a clinical physicist must be in the operating room for any implantation procedure. In addition, it makes use of equipment that is standard in every operating room; therefore, there is virtually no additional cost associated with this procedure.

Quality of Care and Quality of Life for Patients

Our process improves patient quality of care and quality of life significantly as we describe below.

(1) In comparison to traditional computer-aided approaches and other ad hoc heuristic algorithms, the system we developed consistently returns plans with the prescribed dose delivered to 98 percent of the prostate, and it improves conformity ranges (a measure of how closely the prescription isodose curve matches the target tumor contour) from 10–20 percent. The latter improvement translates to a reduction in toxicity and complications to normal tissue exterior to the prostate, including fewer external ulcers, and less bladder and rectum bleeding—side effects that may require surgical corrections.

(2) Clinical evidence shows a significant reduction in average urethra dose and duration of symptom persistence (as we described earlier). Thus, our system results in *fewer patients* requiring medications and urologic intervention for symptom management; those who do experience side effects generally require shorter periods of intervention. This has a *profound impact on both health-care costs and quality of life of the treated patient*.

(3) The procedure uses approximately 20–30 percent fewer seeds and 15 percent fewer needles. Thus, the procedure time is shortened, and it is less invasive because fewer needles are inserted into the body during implantation. This results in faster recovery.

(4) The national distribution of our system and the increasing number of centers performing prostate implants in the United States indicate that its potential clinical significance is far-reaching. Plans can be created rapidly during implantation. The viability of being able to reoptimize in real time based on the actual location of the deposited seeds allows modification of plans when unforeseen difficulties occur during an operation. These modifications can potentially correct any areas of tumor under dosage prior to completion of the brachytherapy procedure (or correction due to implantation error by an inexperienced clinician). In addition, the operator will become more cognizant of what the real-time dose to the urethra and rectum is, and can make dynamic adjustments of the intraoperative plan to ensure that the final dose delivered to these structures remains as low as possible without any compromise of the target coverage. This helps to ensure a uniform quality of care among patients.

(5) The ability to perform (superior) planning intraoperatively results in the elimination of the need for the simulation session. This results in less inconvenience (including time off from work for the simulation and hospital waiting time) for patients.

Accessibility, Training, Quality Control, and Quality Assurance

As is well documented in clinical literature, there is great variability in the experience of human planners who design brachytherapy treatment plans, both within and among institutes, clinics, and hospitals. This variability, combined with the highly complex and labor-intensive nature of traditional computer-aided planning methods, results in huge variability in planning procedures, quality of plans, and ultimately treatment outcomes.

Two significant benefits of the automated computerized planning system that we have developed are the potential removal of the operator-dependent quality of the resulting plans, and its prospect to establish standards and guidelines for cancer treatment quality control and quality assurance. Availability of the system nationwide will significantly reduce the vast variability in planning quality because different clinics will be able achieve the same high-quality plans.

Another benefit relates to its use as a training tool. Unavoidably, as part of the medical training in learning the techniques of seed implantation (not the treatment planning but the actual physical implantation of seeds into the patient's body), mistakes can be made. The advantage of the on-the-fly, multistage reoptimization is that it allows for dynamic dose correction and rapid reoptimization; the resulting partial plan can be amended so as to achieve the desirable clinical properties. The reoptimization thus benefits both the doctor/resident who is learning the physical techniques as well as the patient who still receives a good result because deficiencies in the initial placement can be corrected by later implanted seeds. Psychologically, this allows trainees to focus on mastering the techniques without fearing the result of a bad experience.

As we described above, there is virtually no additional cost associated with this procedure, making it accessible (affordable) to the broad clinical community.

Scientific Advances

The collaborative effort between clinical researchers and OR scientists resulted in scientific advances on two diverse fronts.

Medical Advances

A rapid operator-independent intraoperative treatment planning system provides the groundwork for advancing the technological frontier of brachytherapy. It opens up opportunities to conduct complex clinical investigations that may otherwise be impossible, as evidenced in our study of the tumor shrinkage and seed displacement analysis and 30-day extended dose-control planning (Lee and Zaider 2001a), and on biological MRS-guided dose escalation (Zaider et al. 2000; Lee and Zaider 2004, 2006). The OR modeling paradigm provides great flexibility in modeling the clinical problem realistically, and the rapid solution engine objectively returns the best-possible plans.

The system will serve as a basis for facilitating the standardization of brachytherapy treatment planning in prostate cancer. It also will serve as a foundation on which to base automated computerized treatment planning for general brachytherapy, a process involved in the treatment of a variety of cancers (breast, cervix, esophageal, brain, and sarcoma) throughout the body. *Finally, the system can be used as a tool to carry out research that requires the generation of high-quality, unbiased plans in a timely manner.*

OR Advances

This clinical problem opens up the opportunity for advancing a new and different facet of the OR frontier. Many of the computational integer programming advances in the last 50 years have been strongly motivated by challenges arising from industrial applications. These applications result in large-scale supersparse constraint matrices ($\leq$1 percent) where methodologies now exist that offer good solutions. However, the treatment planning instances have totally dense constraint matrices, and existing solution techniques in commercial MIP solvers are unable to solve them. As a result, we initiated a theoretical investigation that led to the introduction of the concept of conflict hypergraphs and their use in generating cutting planes to assist in the MIP solution process. The resulting computational strategies not only improve solution times for these cancer instances, but also help to solve some intractable, small (10 constraints and 250 variables), yet totally dense market-share instances (Cornuéjols and Dwande 1999, Easton et al. 2003).

Thus, this collaboration advanced the frontiers of knowledge in integer programming. First, conflict hypergraphs provide a rich and complex construct for theoretical investigation of the independent set polytope, a structure embedded as a subsystem in many MIPs. Second, from a computational standpoint, we offer new directions related to separation strategies for hypergraphic structures. In particular, new computational strategies for hypercliques, hyperoddholes, hyperwebs, hyperantiwebs, and parallel cutting-plane algorithms are currently under development. These will aid in the solution of other difficult dense MIP instances—instances that are intractable using currently available strategies. Third, the study of the dense MIP problem is important in its own right in the field of integer programming and OR. Thus, our study establishes a new research frontier to the field of mixed-integer programming where new theory and computational advances can be pursued.

This research and its subsequent clinical advances have attracted much publicity for the OR community. The work was featured in *The New York Times* and *The London Times*, as well as hundreds of medical news publications and newspapers worldwide. In October 2004, it was selected as a feature for the television science news program, Discoveries & Breakthroughs Inside Science, sponsored by the American Institute of Physics and the American Mathematical Society. The three-minute program, entitled "Curing Prostate Cancer," was broadcast on various TV channels nationwide throughout 2005.

Appendix

Mixed-Integer Programming Models

Our treatment models were reported in Gallagher and Lee (1997), Lee et al. (1999a, b), and Lee and Zaider

(2003a). Let x_j be a 0/1 indicator variable for recording placement or nonplacement of a seed in grid position j. Then, the total radiation dose at point P is given by

$$\sum_j D(\|P - X_j\|)x_j, \tag{1}$$

where X_j is a vector corresponding to the coordinates of grid point j, $\|\cdot\|$ denotes the Euclidean norm, and $D(r)$ denotes the dose contribution of a seed to a point r units away. The target lower and upper bounds, L_P and U_P, for the radiation dose at point P can be incorporated with constraint (1) to form dose constraints for the MIP model:

$$\begin{aligned} \sum_j D(\|P - X_j\|)x_j &\geq L_P, \\ \sum_j D(\|P - X_j\|)x_j &\leq U_P. \end{aligned} \tag{2}$$

For each voxel P in each anatomical structure, we associate one binary variable and one continuous variable to capture whether or not the desired dose level is achieved and the deviation of received dose from desired dose. Clinically, it is often desirable to incorporate coverage constraints within the model. For example, the clinician may consider that it is acceptable if, for example, 95 percent of the planning target volume (PTV) receives the prescription dose (*PrDose*). (The PTV includes the visible tumor volume plus an additional margin to encompass potentially diseased cells that are not part of the visible tumor.) We can model such a coverage requirement as follows:

$$\sum_j D(\|P - X_j\|)x_j - r_P = PrDose, \tag{3}$$

$$r_P \leq D^{\text{OD}}_{\text{PTV}} v_P, \tag{4}$$

$$r_P \geq D^{\text{UD}}_{\text{PTV}}(v_P - 1), \tag{5}$$

$$\sum_{P \in \text{PTV}} v_P \geq \alpha|\text{PTV}|. \tag{6}$$

Constraints (3), (4), and (5) must hold for all P in PTV, where PTV is the set of uniformly spaced sample points in the PTV. Here, r_P is a real-valued variable that measures the discrepancy between the prescription dose and actual dose; v_P is a 0/1 variable that captures whether voxel P satisfies the prescription dose bounds or not; α corresponds to the minimum percentage of coverage required (e.g., $\alpha = 0.95$); $D^{\text{OD}}_{\text{PTV}}$ and $D^{\text{UD}}_{\text{PTV}}$ are the maximum overdose and maximum underdose levels tolerated for tumor cells; and |PTV| represents the total number of voxels used to represent the prostate planning volume. If $r_P > 0$, then voxel P receives a sufficient radiation dose to cover the prescribed dose. In this case, $v_P = 1$ and the amount of radiation for voxel P above the prescribed dose is controlled by the maximum allowable overdose constant, $D^{\text{OD}}_{\text{PTV}}$. Similarly, when $r_P < 0$, voxel P is underdosed, and the amount of underdose is limited by $D^{\text{UD}}_{\text{PTV}}$. In this case, $v_P = 0$. Constraint (6) corresponds to the coverage level the clinician desires.

It is typically not possible to satisfy the desired dose constraints at all points simultaneously. This is due in part to the proximity of diseased tissue to healthy tissue. In addition, because of the inverse square distance factor in radiation attenuation, the dose level contribution of a seed to a point less than 0.3 units away is typically larger than the target upper bound for the point. (Hence, the preprocessing techniques commonly mentioned in the integer programming literature cannot be applied directly because this will result in assigning zero to all seed positions.) In our work, we focus on two MIP models and computational strategies that aid in solving the resulting MIP instances.

Model 1

This model identifies a *maximum feasible subsystem* in the proposed linear system. By introducing additional 0/1 variables, one can directly maximize the number of points satisfying the specified bounds. In this case, constraints (2) are replaced by

$$\begin{aligned} \sum_j D(\|P - X_j\|)x_j + N_P(1 - v^L_P) &\geq L_P, \\ \sum_j D(\|P - X_j\|)x_j - M_P(1 - v^U_P) &\leq U_P, \end{aligned} \tag{7}$$

where v^L_P and v^U_P are 0/1 variables, and M_P and N_P are suitably chosen positive constants. If a solution is found such that $v^L_P = 1$, then the right-hand side of the first inequality in (7) is zero; and hence, the lower bound for the dose level at point P is not violated. Similarly, if $v^U_P = 1$, the upper bound at point P is not violated. To find a solution that satisfies as many bound constraints as possible, it suffices to maximize the sum of these additional 0/1 variables;

i.e., maximize $\sum_P (v_P^L + v_P^U)$. In practice, achieving the target dose levels for certain points may be more critical than achieving the target dose levels for certain other points. In this case, one could maximize a weighted sum, $\sum_P (\alpha_P v_P^L + \beta_P v_P^U)$, where the more critical points receive a relatively larger weight. Using a weighted sum was important for the prostate cancer cases. Because there were significantly fewer urethra and rectum points compared to the number of points representing the prostate, to increase the likelihood that the former points achieved the target dose levels, we placed a large weight on the associated 0/1 variables.

The role of the constants M_P and N_P in (7) is to ensure that there will be feasible solutions to the mathematical model. In theory, these constants should be chosen suitably large so that if v_P^L or v_P^U is zero, the associated constraint in (7) will not be violated regardless of how we assign the 0/1 variables x_j. In practice, the choice is driven by computational considerations of the optimization algorithm being used and/or by decisions by the radiation oncologist. For a branch-and-bound algorithm, it is advantageous computationally to assign values that are as tight as possible. The medical expert can guide the selection of the constants by either assigning absolute extremes on acceptable radiation dose levels delivered to each point (note that $U_P + M_P$ is the absolute maximum dose level that will be delivered to point P under the constraints in (7), and $L_P - N_P$ is the absolute minimum), or by estimating the number of seeds needed for a given plan. In the latter case, if the number of seeds needed is estimated to be between k_1 and k_2 ($k_1 \le k_2$), for example, then the constant N_P can be taken to be L_P minus the sum of the smallest k_1 of the values $D(\|P - X_j\|)$, and the constant M_P can be taken to be the sum of the largest k_2 such values minus U_P. Selection in this fashion will ensure that no plan having between k_1 and k_2 seeds will be eliminated from consideration.

Model 2

An alternative model uses continuous variables to capture the deviations of the dose level at a given point from its target bounds and minimizing a weighted sum of the deviations. In this case, we replace constraints (2) by constraints of the form

$$\begin{aligned} \sum_j D(\|P - X_j\|)x_j + y_P^L &\ge L_P, \\ \sum_j D(\|P - X_j\|)x_j - y_P^U &\le U_P, \end{aligned} \tag{8}$$

where y_P^L and y_P^U are nonnegative continuous variables. The objective for this model takes the form minimize $\sum_P (\alpha_P y_P^L + \beta_P y_P^U)$, where α_P and β_P are nonnegative weights selected according to the relative importance of satisfying the associated bounds. For example, weights associated with an upper bound on the radiation dose for points in a neighboring healthy organ may be given a relatively larger magnitude than weights associated with an upper bound on the dose level for points in the diseased organ.

Model Variations and Other Side Constraints

Both models allow the incorporation of alternative seed types. There are a variety of radioactive sources that are used for brachytherapy—these include palladium-103, iodine-125, which are commonly used for treating prostate cancer, and cesium-137, iridium-192, and gold-198, each of which has its own set of exposure rate constants. At this time, however, a single-seed type and radiation strength are used in a given treatment plan. This fact is, in part, due to the difficulty of designing treatment plans with multiple strength and seed types as well as identifying multiple-seed types in postdosimetry analysis. The allowance of multiple strength and seed types can easily be incorporated into the MIP framework—one need only modify the total dose level expression (1) as

$$\sum_j \sum_i D_i(\|P - X_j\|)x_{ij}. \tag{9}$$

Here, x_{ij} is the indicator variable for placement or nonplacement of a seed of type i in grid location j, and $D_i(r)$ denotes the dose level contribution of a seed of type i to a point r units away. In this case, a constraint restricting the number of seeds implanted at grid point j is also needed: $\sum_i x_{ij} \le 1$.

To aid in reducing urinary and rectal toxicity, our approach involves the imposition of strict dosimetric-volume bounds on the urethra and rectum in both MIP models. Besides the basic dosimetric constraints

and dose-volume constraints to ensure sufficient coverage to the tumor volume, we also incorporate other physical constraints that the clinicians desire into our MIP models. One could incorporate constraints to control the percentage of each tissue structure satisfying specified target bounds. Alternatively, one could—if desired—constrain the total number of seeds and/or needles used. Note also that one can ensure that target dose bounds at specific points are satisfied by fixing the associated "feasibility" variables (v_P^L, v_P^U, y_P^L, y_P^U) to appropriate values.

Computational Strategies

We note that unlike most of the industrial applications in which the MIP instances contain sparsely populated nonzero entries in the constraint matrices, the resulting MIP instances for treatment optimization have mostly dense matrices. Furthermore, the magnitudes of the coefficients range from the order of tens to tens of thousands. Below we highlight some specialized strategies that have shown to be effective in improving the tractability of the resulting instances. The details of the computational analysis were reported in Lee and Zaider (2003a).

Matrix Reduction and Approximation Scheme

Motivated by the dense constraint matrices and range in the magnitudes in the nonzero entries, we investigated a matrix reduction and perturbation approach. The reduction scheme partitions the constraint matrix into two submatrices, based on the magnitude of the coefficients. We perturb the right-hand side to compensate for the change in the matrix coefficients. Specifically, we are interested in a dense MIP instance of the following form:

$$\begin{aligned} Ax - Ny &\geq L, \\ Ax + Mz &\leq U, \qquad \text{(S)} \\ x \in Z_+^n, \quad y \in \Re_+^p, \quad z &\in \Re_+^q, \end{aligned}$$

where A is an $m \times n$ nonnegative dense matrix, and N and M are $m \times p$ and $m \times q$ nonnegative (sparse) matrices, respectively. Let $P^S = \text{conv}\{(x, y, z)\ Ax - Ny \geq L,\ Ax + Mz \leq U,\ x \in Z_+^n,\ y \in \Re_+^p,\ z \in \Re_+^q\}$. For the sake of presentation, we assume that y and z are continuous variables. However, the method we described below also works when they are restricted to assume integer values.

Definition. For a chosen $\delta > 0$, split the matrix A as $A = A^1 + A^2$, where

$$a_{ij}^1 = \begin{cases} a_{ij} & \text{if } a_{ij} \geq \delta, \\ 0 & \text{otherwise,} \end{cases} \quad \text{and} \quad a_{ij}^2 = \begin{cases} a_{ij} & \text{if } a_{ij} < \delta, \\ 0 & \text{otherwise.} \end{cases}$$

Let A_i denote the ith row of matrix A, and let $\bar{x}$ and $\hat{x}$ solve the following linear programs, respectively:

$$\max_{\{i:\, A_i^2 \neq 0\}} \max\{A_i^2 x:\, x \in P^S\} \quad \text{and} \quad \min_{\{i:\, A_i^2 \neq 0\}} \min\{A_i^2 x:\, x \in P^S\}.$$

Consider the following two systems:

(1) The system

$$\begin{aligned} A^1 x - Ny &\geq L - A^2 \bar{x}, \\ A^1 x + Mz &\leq U - A^2 \hat{x}, \\ x \in Z_+^n, \quad y \in \Re_+^p, \quad z &\in \Re_+^q, \end{aligned}$$

is called a *δ-reduction* for (S). It is easy to check that if (x, y, z) is feasible for (S), then it is feasible for its δ-reduction. The converse does not hold. Clearly, if $x_j \in [\alpha_j, \beta_j]$, $j = 1, \ldots, n$, we can approximate $\bar{x}_j$ and $\hat{x}_j$ by β_j and α_j, respectively.

(2) Let $\varepsilon \in Z_+^n$. The system

$$\begin{aligned} A^1 x - Ny &\geq L - A^2 \varepsilon, \\ A^1 x + Mz &\leq U - A^2 \varepsilon, \\ x \in Z_+^n, \quad y \in \Re_+^p, \quad z &\in \Re_+^q, \end{aligned}$$

is called a *δ-reduction-ε-approximation* for (S) if $A^2 \hat{x} \leq A^2 \varepsilon \leq A^2 \bar{x}$.

We caution that applying these schemes to the MIP instances is difficult. In particular, the selection of δ and ε is empirical and problem dependent because the coefficients in each row of the dosimetric constraint matrix vary greatly. In some rows, the coefficients are distributed in the range from tens to hundreds, whereas in others there are various coefficients (fewer than 10 percent) that have magnitudes in the hundreds of thousands and tens of thousands, and the rest range from tens to thousands. Here, we describe an implementation using the dosimetric constraints for Model 1:

$$\begin{aligned} \sum_{j=1}^n D(\|P - X_j\|) x_j + N_P(1 - v_P^L) &\geq L_P, \\ \sum_{j=1}^n D(\|P - X_j\|) x_j - M_P(1 - v_P^U) &\leq U_P. \end{aligned}$$

To select δ, one pass is made through the constraint matrix to evaluate the distribution of the nonzeros in each row. For row i, we calculate the average of the largest 5 percent of the nonzero coefficients, $\text{ave}^{\max}$. Initialize $K = 0$. The set K will be populated with the set of indices selected in a nondecreasing manner, starting from the smallest nonzero coefficient. We continue to place an index into K until $\text{ave}\{D(\|P - X_j\|) : j \in K\}$ is approximately equal to $\gamma * \text{ave}^{\max}$, or until the cardinality of the set K exceeds 50 percent of the total number of nonzeros in the given row. We then assign $\delta_i = \max\{D(\|P - X_j\|): j \in K\}$ and $\delta = \max\{\delta_i\}$. For a row with coefficients exceeding a magnitude of 10,000, we set $\gamma = 0.5$ percent. For all other rows, we increase this value gradually with the amount of decrease in the magnitude of the coefficients.

Assuming there are m rows for each of the two classes of dosimetric constraints, the complexity of the search includes $O((n+1)\log(n+1))$ operations for sorting the nonzero coefficients for each row, and $O(m(n+1)\log(n+1))$ operations to set up the δ-reduction system.

Penalty-Based Adaptive Primal Heuristic Procedure
The heuristic procedure is an LP-based primal heuristic in which at each iteration, some binary variables are set to one and the corresponding linear program is resolved. The procedure terminates when the linear program returns an integer feasible solution or when it is infeasible. In the former case, reduced-cost fixing is performed at the root node, as well as locally on each of the branch-and-bound nodes.

Again focusing on Model 1, let x^{LP} be an optimal solution of some linear program relaxation at a branch-and-bound node. (For simplicity of notation, the variables v_P^L and v_P^U are included as part of x^{LP}.) At the start of the heuristic procedure, penalties, p_j, for all variables are set to zero. Let $U = \{j: x_j^{\text{LP}} = 1\}$ and $F = \{j: 0 < x_j^{\text{LP}} < 1\}$. The procedure works by first setting $x_j = 1$ for all $j \in U$. For each $j \in F$ corresponding to a grid point j with coordinates X_j, the penalty on x_j is updated according to the formula

$$p_j = \sum_{\substack{k:\, x_k^{\text{LP}}=1 \\ k \text{ a grid point}}} \frac{1}{\|X_k - X_j\|}.$$

For all other $j \in F$ (i.e., j corresponding to v_P^L and v_P^U), the penalties remain at value zero. Let $x^{\max} = \max\{x_j^{\text{LP}}: j \in F\}$ and $\varepsilon > 0$. In nondecreasing order of p_js, the variables in F are set to one if $x_j^{\text{LP}} \geq x^{\max} - \varepsilon$. Because penalties for fractional v_P^L and v_P^U variables are always set to zero, these variables are always considered first for setting to one. For every binary variable that is set to one, logical implication (probing) (Bixby and Lee 1993, 1998; Savelsbergh 1994) is performed to avoid conflicts in variable fixing. The value ε is chosen dynamically at each iteration so that approximately 10 percent of the fractional variables are set to one, a strategy that appears to work well empirically for our MIP instances.

Penalty Branching Strategy
Branching variables are selected based on pseudocosts as well as penalties. Let $\varepsilon > 0$ be given, and let $K = \{j: \varepsilon < x_j^{\text{LP}} < 1 - \varepsilon\}$. One can control the size of K by choosing ε so that $|K|$ reaches a certain percentage with respect to $|F|$. For each $k \in K$, the degradations U_k and D_k in the objective value when branching with x_k set to one and zero, respectively, are calculated, and the penalties p_k are computed in the same manner as we described in the previous section. The branching variable is chosen as that value with the maximum penalty-weighted degradation, which is computed as $\max_{\{k \in K\}}\{D_k + U_k/(p_k + 1)\}$. The values U_k and D_k can be calculated exactly by solving the respective linear programs, or can be approximated by performing only a fixed number of simplex iterations. The approximation strategy helps to control the required computational effort. We report results based on performing 50 simplex iterations using the steepest-edge strategy.

Acknowledgments
This work was partially supported by the National Science Foundation and the Whitaker Foundation. We thank the Edelman reviewers for their valuable comments on an earlier version of this manuscript. We thank Michael J. Zelefsky for his invaluable support.

References

American Cancer Society. 2006. Cancer facts and figures. American Cancer Society, Atlanta.

Anderson, L. L. 1993. Planning optimization and dose evaluation in brachytherapy. *Sem. Radiation Oncology* **3** 290–300.

Bixby, R. E., E. K. Lee. 1993. Solving a truck dispatching scheduling problem using branch-and-cut. Doctoral dissertation, Rice University, Houston.

Bixby, R. E., E. K. Lee. 1998. Solving a truck dispatching scheduling problem using branch-and-cut. *Oper. Res.* **46**(3) 355–367.

Blasko, J. C., H. Ragde, R. W. Luse, J. E. Sylvester, W. Cavanagh, P. D. Frimm. 1996. Should brachytherapy be considered a therapeutic option in localized prostate cancer? *Urologic Clinics North Amer.* **23** 633–650.

Cornuéjols, G., M. Dwande. 1999. A class of hard small 0-1 programs. *INFORMS J. Comput.* **11**(2) 205–210.

Easton, T., K. Hooker, E. K. Lee. 2003. Facets of the independent set polytope. *Math. Programming B* **98** 177–199.

Gallagher, R. J., E. K. Lee. 1997. Mixed integer programming optimization models for brachytherapy treatment planning. D. R. Masys, ed. *Proc. 1997 Amer. Medical Informatics Assoc. Annual Fall Sympos.*, Nashville, TN, 278–282.

Kleinberg, L., K. Wallner, M. Zelefsky, V. E. Arterbery, Z. Fuks, L. Harrison. 1994. Treatment related symptoms during the first year following transperineal ^{125}I prostate implantation. *Internat. J. Radiation Oncology Biol. Phys.* **28** 985–990.

Kutcher, G. J., C. Burman. 1989. Calculation of complication probability factors for non-uniform normal tissue irradiation: The effective volume method. *Internat. J. Radiation Oncology Biol. Phys.* **16** 1623–1630.

Lee, E. K., S. Maheshwary. 2008. Facets of conflict hypergraphs. *Math. Oper. Res.* In review.

Lee, E. K., M. Zaider. 2001a. Determining an effective planning volume for permanent prostate implants. *Internat. J. Radiation Oncology Biol. Phys.* **49**(4) 1197–1206.

Lee, E. K., M. Zaider. 2001b. Intraoperative iterative treatment-plan optimization for prostate implants. *2nd Internat. Innovative Solutions for Prostate Cancer Care Meeting*, Coronado Island, CA, 32–33.

Lee, E. K., M. Zaider. 2003a. Mixed integer programming approaches to treatment planning for brachytherapy—Application to permanent prostate implants. *Ann. Oper. Res.* **119** 147–163.

Lee, E. K., M. Zaider. 2003b. Intra-operative dynamic dose optimization in permanent prostate implants. *Internat. J. Radiation Oncology Biol. Phys.* **56**(3) 854–861.

Lee, E. K., M. Zaider. 2004. Incorporating biological metabolite information within treatment of prostate carcinoma. *Internat. J. Radiation Oncology Biol. Phys.* **60**(1) S370–S371.

Lee, E. K., M. Zaider. 2006. Incorporating biological metabolite information within treatment of prostate carcinoma and analysis of dose escalation effect. *Internat. J. Radiation Oncology Biol. Phys.* **66**(3) S572–S573.

Lee, E. K., R. Gallagher, M. Zaider. 1999a. Planning implants of radionuclides for the treatment of prostate cancer: An application of mixed integer programming. *Optima, Math. Programming Soc. Newsletter* **61** 1–10.

Lee, E. K., R. J. Gallagher, D. Silvern, C. S. Wuu, M. Zaider. 1999b. Treatment planning for brachytherapy: An integer programming model, two computational approaches and experiments with permanent prostate implant planning. *Phys. Med. Biol.* **44** 145–165.

Lyman, J. T. 1985. Complication probabilities as assessed from dose-volume histograms. *Radiation Res.* **104** S13–S19.

Moerland, M. A., H. K. Wijrdeman, R. Beersma, C. J. Bakker, J. J. Battermann. 1997. Evaluation of permanent I-125 prostate implants using radiography and magnetic resonance imaging. *Internat. J. Radiation Oncology Biol. Phys.* **37**(4) 927–933.

New York Times. 2001. Computerized treatment may help prostate cancer. (February 20).

New York Times. 2006. Profit and questions as doctors offer prostate cancer therapy. (December 1) A1.

Prestidge, B. R., W. S. Bice, E. J. Kiefer, J. J. Prete. 1998. Timing of CT-based post-implant assessment following permanent transperineal prostate brachytherapy. *Internat. J. Radiation Oncology Biol.* **40**(5) 1111–1115.

Savelsbergh, M. W. P. 1994. Preprocessing and probing for mixed integer programming problems. *ORSA J. Comput.* **6** 445–454.

Silvern, D. A. 1998. Automated OR prostate brachytherapy treatment planning using genetic optimization. Doctoral dissertation, Columbia University, New York.

Silvern, D., E. K. Lee, R. J. Gallagher, L. G. Stabile, R. D. Ennis, C. R. Moorthy, M. Zaider. 1997. Treatment planning for permanent prostate implants: Genetic algorithm versus integer programming. *Medical Biol. Engrg. Comput.* **35** 850.

Sloboda, R. S. 1992. Optimization of brachytherapy dose distributions by simulated annealing. *Medical Phys.* **19** 955–964.

Wallner, K., J. Roy, L. Harrison. 1996. Tumor control and morbidity following transperineal iodine 125 implantation for stage T1/T2 prostatic carcinoma. *J. Clinical Oncology* **14** 449–453.

Wallner, K., H. Lee, S. Wasserman, M. Dattoli. 1997. Low risk of urinary incontinence following prostate brachytherapy in patients with a prior transurethral prostate resection. *Internat. J. Radiation Oncology Biol. Phys.* **37** 565–569.

Waterman, F. M., A. P. Dicker. 1999. Effect of postimplant edema on the rectal dose in prostate brachytherapy. *Internat. J. Radiation Oncology Biol. Phys.* **45** 571–576.

Waterman, F. M., N. Yue, B. W. Corn, A. P. Dicker. 1998. Edema associated with I-125 or Pd-103 prostate brachytherapy and its impact on postimplant dosimetry: An analysis based on serial CT aquisition. *Internat. J. Radiation Oncology Biol. Phys.* **41** 1069–1077.

Waterman, F. M., N. Yue, S. Reisinger, A. P. Dicker, B. W. Corn. 1997. Effect of edema on the postimplant dosimetry of an I-125 prostate implant: A case study. *Internat. J. Radiation Oncology Biol. Phys.* **38** 335–339.

Wei, J. T., R. L. Dunn, H. M. Sandler, P. W. McLaughlin, J. E. Montie, M. S. Litwin, L. Nyquist, M. G. Sanda. 2002. Comprehensive comparison of health-related quality of life after contemporary therapies for localized prostate cancer. *J. Clinical Oncology* **20**(2) 557–566.

Yu, Y., M. C. Schnell. 1996. A genetic algorithm for optimization of prostate implants. *Medical Phys.* **23** 1085–1091.

Yue, N., A. P. Dicker, R. Nath, F. M. Waterman. 1999a. The impact of edema on planning 125I and 103Pd prostate implants. *Medical Phys.* **26**(5) 763–767.

Yue, N., A. P. Dicker, B. W. Corn, R. Nath, F. M. Waterman. 1999b. A dynamic model for the estimation of optimum timing of computed tomography scan for dose evaluation of I-125 or Pd-103 seed implant of prostate. *Internat. J. Radiation Oncology Biol. Phys.* **43** 447–454.

Zaider, M. 2003. Aspects of brachytherapy physics. S. A. Leibel, T. L. Phillips, eds. *Textbook of Radiation Oncology*, 2nd ed. Saunders, Philadelphia.

Zaider, M., M. J. Zelefsky, E. K. Lee, K. L. Zakian, H. I. Amols, J. Dyke, G. Cohen, Y. C. Hu, A. K. Endi, C. S. Chui, J. A. Koutcher. 2000. Treatment planning for prostate implants using magnetic resonance spectroscopy imaging. *Internat. J. Radiation Oncology Biol. Phys.* **47** 1085–1096.

Zelefsky, M. J., W. F. Whitmore. 1997. Long term results of retropubic permanent 125-iodine implantation of the prostate for clinically localized prostatic cancer. *J. Urology* **158** 23–29.

Zelefsky, M. J., T. Hollister, A. Raben, S. Matthews, K. E. Wallner. 2000a. Five-year biochemical outcome and toxicity with transperineal CT-planned permanent I-125 prostate implantation for patients with localized prostate cancer. *Internat. J. Radiation Oncology Biol. Phys.* **47**(5) 1261–1266.

Zelefsky, M. J., Y. Yamada, G. N. Cohen, A. Shippy, H. Chan, D. Fridman, M. Zaider. 2007. Five-year outcome of intraoperative conformal permanent I-125 interstitial implantation for patients with clinically localized prostate cancer. *Internat. J. Radiation Oncology Biol. Phys.* **67**(1) 65–70.

Zelefsky, M. J., Y. Yamada, G. Cohen, E. S. Venkatraman, A. Y. C. Fung, E. Furhang, D. Silvern, M. Zaider. 2000b. Postimplantation dosimetric analysis of permanent transperineal prostate implantation: Improved dose distribution with an intraoperative computer optimized conformal planning technique. *Internat. J. Radiation Oncology Biol. Phys.* **48** 601–608.

Zelefsky, M. J., Y. Yamada, C. Marion, S. Sim, G. Cohen, L. Ben-Porat, D. Silvern, M. Zaider. 2003. Improved conformality and decreased toxicity with intraoperative computer-optimized transperineal ultrasound-guided prostate brachytherapy. *Internat. J. Radiation Oncology Biol. Phys.* **55**(4) 956–963.

Zelefsky, M. J., K. E. Wallner, C. C. Ling, A. Raben, T. Hollister, T. Wolfe, A. Grann, P. Gaudin, Z. Fuks, S. A. Leibel. 1999. Comparison of the 5-year outcome and morbidity of three-dimensional conformal radiotherapy versus transperineal permanent iodine-125 implantation for early-stage prostatic cancer. *J. Clinical Oncology* **17**(2) 517–522.